[6]R. J. Elliott, Phys. Rev. 108, 1383 (1957).
[7]G. D. Mahan and B. Segall, in Proceedings of the Conference on II-VI Compounds (to be published).
[8]For small values of $\kappa$ one may approximate $L(\kappa) = \kappa^2[1+O(\kappa)]$. This approximate result was derived previously in Ref. 5 and used by Hopfield and Worlock (Ref. 2). Unfortunately, $\kappa$ is large enough such that this approximation is not very accurate in the alkali halides.
[9]J. Ramamurti and K. Teegarden, Phys. Rev. 145, 698 (1965).
[10]G. D. Mahan, to be published.

## OPTICAL PROBING OF MAGNETOELASTIC WAVES

Archibald W. Smith
IBM Watson Research Center, Yorktown Heights, New York
(Received 21 December 1968)

The diffraction of a light beam is used to study the propagation of transverse magnetoelastic waves generated in a bar of yttrium iron garnet by an rf magnetic field. For the first time, waves are observed on the lower as well as on the upper branch of the magnetoelastic dispersion curves.

In the past, the behavior of magnetoelastic (ME) waves has been inferred from microwave signals generated at a turning point by the ME waves.[1-3] In the present work, the diffraction of a light beam by transverse ME waves is used to study their propagation throughout the volume of an yttrium iron garnet (YIG) bar. We directly observe, for the first time, a ME wave traveling through the center of the YIG bar which is on the lower branch of the ME dispersion curves. This wave must arise by interbranch transfer from the upper branch, since direct generation is not possible on the lower branch. A wave traveling toward the end of the bar on the upper branch is also found, which is reflected back to the turning point, in agreement with previous work. The ME waves are excited by an rf magnetic field; some results for the case of elastic excitation on the upper branch have been given earlier.[4-6]

The geometry of the experiment is shown in Fig. 1. The YIG bar was 10 mm long and $3\times3$ mm$^2$ in cross section. The bar axis was the [001] cubic direction, and the magnetic field was applied parallel to this direction. Transverse ME waves of frequency $\omega_m$ and wave number $k_m$ were excited along the bar axis by placing an electrode such as a ball or half-loop against one end of the bar. The electrode structure was resonated with a coaxial stub tuner ($Q \approx 200$). Diffraction was observed under Bragg conditions[7]; the Bragg angle $\theta_B$ is given by $\sin\theta_B = k_m/2k_0$, where $k_0$ is the optical wave number. The laser beam was focused in the bar with a 15-cm focal length lens, and could be positioned anywhere in the bar except near the ends. Because of the focusing, the angular resolution in $\theta_B$ was only $\pm\frac{1}{3}°$. The ME frequency was 1.1 GHz, the laser wavelength 1.15 $\mu$, and $\theta_B = \theta_{BE} = 9.5°$ in the elastic limit. The maximum rf power of approximately 300 W was much larger than that used in previous experiments. The strongest diffracted signals were observable down to a minimum of 5 W, with little change in behavior.

A relation exists between the direction of the ME wave and the polarization of the laser beam for maximum diffracted intensity. If the relative directions of the ME wave and laser beam are such that the diffracted beam is Doppler shifted upwards in frequency[7] by $\omega_m$, then the laser must be polarized perpendicular to the plane of the diffraction, as illustrated in Fig. 1. If $k_m$ is reversed, the laser polarization must be parallel to the plane of the diffraction. This relation enables the direction of an unknown wave to be determined from polarization measurements instead of moving the laser beam to measure the delay time.

The polarization effects result from the combination of the spin wave and elastic contributions to the diffraction.[5,8] The diffracted am-

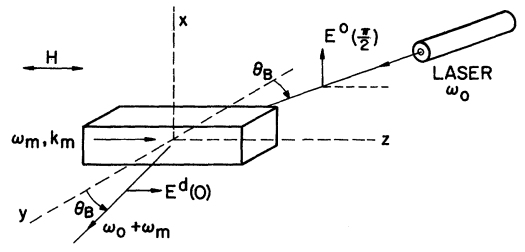


FIG. 1. Experimental arrangement and coordinate system. Transverse ME waves are excited by an rf magnetic field in the bar, and are detected by diffraction of the laser beam.

plitude is proportional to $\varphi_F = \varphi_F{}^0\alpha$ and $\varphi_P = \varphi_P{}^0\epsilon$, respectively, for the two contributions, where $\alpha$ is the fractional spin-wave magnetization, $\epsilon$ the shear strain, $\varphi_F{}^0$ the dc Faraday rotation, and $\varphi_P{}^0 = \frac{1}{2}n^3 p_{44} k_0$. From previous work, $\varphi_F{}^0 \approx 4.7$ rad/cm at 1.15 $\mu$, the index of refraction $n \approx 2.3$, the photoelastic constant[9] $p_{44} = 0.04$, and therefore $\varphi_P{}^0 \approx 1.4\times10^4$ rad/cm. An analysis of the diffraction gives the following result for the laser polarization parallel (0) and perpendicular ($\frac{1}{2}\pi$) to the plane of diffraction:

$$E^d(\tfrac{1}{2}\pi) = \tfrac{1}{2}C(\varphi_P \mp \varphi_F)E^0(0),$$

$$E^d(0) = \tfrac{1}{2}C(\varphi_P \pm \varphi_F)E^0(\tfrac{1}{2}\pi), \quad (1)$$

where $E^0$ and $E^d$ are the incident and diffracted optical amplitudes, respectively, $C$ is a constant, and the orientation of the polarization is measured from the plane of diffraction. The upper and lower signs refer to the up- and down-shifted frequency cases, respectively. The sign changes have been verified experimentally for ME waves traveling in known directions.

If the laser polarization is oriented at $\frac{1}{4}\pi$ to the plane of diffraction, the result obtained is

$$E^d(\tfrac{1}{4}\pi) = C\varphi_P E^0(\tfrac{1}{4}\pi),$$

$$E^d(\tfrac{3}{4}\pi) = C\varphi_F E^0(\tfrac{1}{4}\pi). \quad (2)$$

As can be seen, the photoelastic and Faraday rotation contributions are at right angles and may be separated by using a polarizer in the diffracted beam. Thus the ratio $\varphi_F/\varphi_P = \varphi_F{}^0\alpha/\varphi_P{}^0\epsilon$ can be determined. For small amplitude signals under the present conditions, $\alpha$ and $\epsilon$ are related by[1,2]

$$\frac{\alpha}{\epsilon} = \frac{\rho(\omega_m{}^2 - c_t{}^2 k_m{}^2)}{bk_m{}^2}, \quad (3)$$

where $k_m$ is a function of the internal field, $b$ is the magnetoelastic interaction constant, $\rho$ is the density, and $c_t$ is the transverse elastic velocity.

The ME waves observed in the bar will now be described. If the laser beam is positioned in the half of the bar closest to the electrode, strong diffracted signals are obtained at the elastic limit $\theta_{BE} = 9.5°$ when $H_i$ is approximately $\omega_m/\gamma$ at the laser beam. The strongest ME wave propagates toward the electrode end of the bar (see Fig. 2). Since the bar has a field maximum at the center, this is a wave generated on the upper branch at a turning point ($H_i = \omega_m/\gamma$) and propagating into a low-field region, in agreement with previous work.[1-3] If the wave is followed toward the end of the bar by moving the laser beam, the diffracted signal drops rapidly by a factor of 1/30. The wave reflects from the end of the bar and returns to the generation point, where the diffracted signal increases by a factor of 3 to 10, depending on the position in the bar. At this point a microwave signal is emitted, in agreement with previous microwave studies. The average velocity is about 10% less than the elastic velocity $c_t$. The diffracted signals are transient in nature. They decay in 0.3 $\mu$sec, which is about equal to the spin-lattice relaxation time[10] for $k_m \approx 10^4$ cm$^{-1}$.

An anomalous observation for this wave is that after it leaves the generation point, it can be observed over a range of $\theta_B$ from 9.5° to 7.5°, and the ratio $\varphi_F/\varphi_P$ increases (see Fig. 2). This is especially noticeable after the wave is reflected from the end and indicates that the wave is becoming more magnetic. The range of $\theta_B$ gives a range of $k$ values from $1.8\times10^4$ to $1.4\times10^4$ cm$^{-1}$. We would expect the wave to become more elastic as it travels into the low-field end zone with $\theta_B = \theta_{BE}$ and $\varphi_F/\varphi_P$ approaching zero. A probable reason for the anomalous behavior is found in the large divergence of the wave: about 9° at the generation point, decreasing quickly to 2° as it travels toward the end (the divergence is tak-

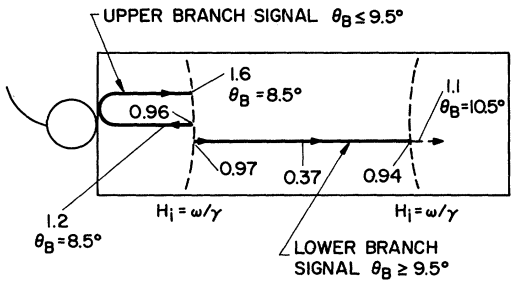


FIG. 2. Schematic view of ME waves observed in the bar. All waves occupy a region about 1 mm high in the center of the bar, but have been displaced vertically in the figure for clarity. The numbers are values of $\varphi_F/\varphi_P$, measured at $\theta_B = 9.5°$ unless marked otherwise.

en as $\Delta\varphi/n$, where $\Delta\varphi$ is the rotation of the bar between the points of half-maximum intensity, with $\theta_B$ fixed). Since the dispersion curves shift upward if the wave travels at an angle $\theta_k$ to $H_i$, the divergent rays effectively see a range of internal fields given by $H_i(\text{eff}) = \omega_m/\gamma - 2\pi M\theta_k^2$ for $\theta_k \ll 1$. The observed range of $k_m$ is consistent with the observed divergence of 2°.

Returning now to the original position in the bar, a second strong signal is observed at $\theta_{BE}$ when the turning point is at the laser. This wave travels through the center of the bar to the conjugate turning point at the other end, where it disappears (see Fig. 2). The average velocity is again somewhat less than $c_t$. Since this wave propagates in a high-field region ($H_i > \omega_m/\gamma$), it must be on the lower branch. This is confirmed by an optical polarization analysis shown in Fig. 3. The relative contribution of the spin wave to the diffraction decreases near the center, as expected for a wave on the lower branch. It should be noted that a considerable increase in the spin-wave magnetization is possible before $\theta_B$ deviates from $\theta_{BE}$ more than the angular resolution of $\pm\frac{1}{3}°$.[4] Thus the polarization analysis can be carried out over a range of $\varphi_F/\varphi_P$ from 0 to about 1 without a resolvable change in $\theta_B$.

As this wave disappears, a weak diffracted signal is observed traveling beyond the conjugate turning point with $\theta_B$ spread over the range 9.5°-11.5°, as indicated by the small dashed arrow in Fig. 2. This is consistent with a lower branch wave propagating into the low-field end region, where it should rapidly become a spin wave with high attenuation.

It will be seen from Fig. 3 that the net diffracted intensity increases close to the turning points. A similar effect is observed for the upper branch wave. This is due to the decrease in group velocity in the crossover region of the ME dispersion curves, which increases the energy density of the wave. The divergence of the wave on the lower branch increases from 5° at the generation point to 9° at the conjugate position. At the same time the width in the $x$ direction (Fig. 1) decreases from 1.5 to 1.0 mm, so there is a slight focusing effect here.[11] The divergence of the beam has little effect on the lower branch wave since it becomes more elastic in nature as $\theta_k$ increases.

There is a systematic difference in the magnetic field for maximum intensity of the waves

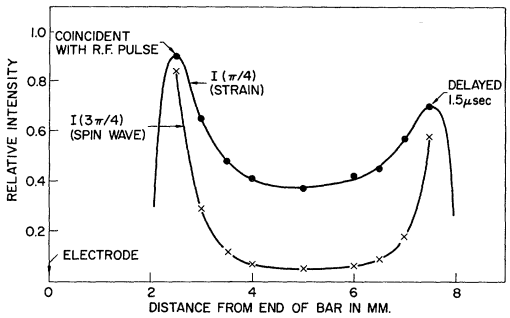


FIG. 3. Optical polarization analysis of the lower branch wave at $\theta_B = 9.5°$, fixed applied field, and laser polarization at $\frac{1}{4}\pi$ to the diffraction plane. Diffracted signals with the output polarizer at $\frac{1}{4}\pi$ and $\frac{3}{4}\pi$ are due to strain and spin-wave magnetization, respectively.

on the upper and lower branches: The upper branch signal is strongest when $H_i$ is about 20 Oe below $\omega_m/\gamma$. Thus it must be generated slightly toward the center of the bar from the laser position, and is partially converted to an elastic wave before it gives the strong diffracted signal at $\theta_{BE}$. It should be noted that the field settings for maximum intensity are about 20 Oe wide because the internal field varies along the laser beam in the bar.

Since only the upper branch signal can be directly generated, the observed lower branch signal must arise by interbranch transfer in the crossover region of the ME dispersion curves. On the basis of previous theoretical work, this transfer should be small unless the field gradient exceeds a value[2] of $H_i' = \pi b^2\omega_m/c_t^3 M\rho$, which is about $2\times10^4$ Oe/cm for YIG at 1.1 GHz. The gradients in the present bar are much less than this; for example, 2.5 mm from the end of the bar $H' \approx 6\times10^2$ Oe/cm. On the other hand, the lower branch signal varies from roughly $\frac{1}{4}$ to $\frac{3}{4}$ of the upper branch signal, depending on the position in the bar and on the particular electrode structure; so there is a large transfer of power. This ratio does not follow the variation of $H'$ along the bar. A possible reason for these discrepancies is that large-amplitude, transient signals are being observed, whereas the calculations[2] assume small-amplitude, steady-state values. It would be desirable to have a fuller understanding of the interbranch transfer mechanism in order to explain the present results.

I thank N. S. Shiren and J. C. Slonczewski for helpful discussions, and A. J. Landon for technical assistance.

[1]W. Strauss, Proc. IEEE 53, 1485 (1965).
[2]E. Schlömann, R. I. Joseph, and T. Kohane, Proc. IEEE 53, 1495 (1965).
[3]B. A. Auld, Proc. IEEE 53, 1517 (1965).
[4]A. W. Smith, Appl. Phys. Letters 11, 7 (1967).
[5]A. W. Smith, to be published.
[6]R. W. Dixon, J. Appl. Phys. 38, 3634 (1967).
[7]C. F. Quate, C. D. W. Wilkinson, and D. K. Winslow, Proc. IEEE 53, 1604 (1965).
[8]B. A. Auld and D. A. Wilson, J. Appl. Phys. 38, 3331 (1967).
[9]R. W. Dixon and H. Matthews, Appl. Phys. Letters 10, 195 (1967).
[10]R. C. LeCraw and E. G. Spencer, J. Phys. Soc. Japan 17, 401 (1962).
[11]B. A. Auld, IEEE Trans. Sonics Ultrasonics SU-13, 92 (1966).

# THEORETICAL TREATMENT OF THE ELASTIC AND INELASTIC SCATTERING OF 1-GeV PROTONS FROM NUCLEI*

H. K. Lee
Duquesne University, Pittsburgh, Pennsylvania

and

H. McManus
Michigan State University, East Lansing, Michigan
(Received 22 December 1967)

Recently data have become available on the elastic and inelastic scattering of 1-GeV protons.[1] The elastic scattering data on $^{16}O$ and $^{12}C$ have been analyzed in terms of an empirical optical potential[2] and the inelastic scattering in terms of the Blair diffraction model.[3] The elastic scattering from $^4He$, which is quite different, has been analyzed in terms of the high-energy scattering theory of Glauber.[4] In the present note a calculation is presented using the WKB-impulse approximation for both the elastic and inelastic scattering of 1-GeV protons from $^{12}C$ and $^{16}O$ using microscopic form factors for the inelastic scattering from excited states of $^{12}C$ and $^{16}O$.

For the elastic scattering, the charge distribution was taken from the old analysis of electron scattering data[5] to be of the form $\rho_C(r) = \rho_0(1+\mu r^2)e^{-\alpha r^2}$. The optical potential was then written in terms of the nucleon-nucleon forward-scattering amplitude $A(0)$:

$$V_{\text{opt}} = -(2\pi N/E)A(0)\rho_C(r). \quad (1)$$

The nucleon-nucleon scattering amplitude was taken to be the same as used by Bassel and Wilkin,[4]

$$A(q) = [k\sigma(i-0.325)/4\pi]e^{-\frac{1}{2}a^2|t|}, \quad (2)$$

with $a = 5.23\ (\text{GeV}/c)^{-2}$ and $\sigma = \frac{1}{2}(\sigma_{pp}+\sigma_{pn}) = 43.3$ mb as a function of momentum transfer $q^2 = -t$. With this form for the scattering amplitude, (1) should be a good approximation, since the variation of the amplitude (2) with momentum transfer is very much the same as the proton electromagnetic form factor, so that corrections to (1) for the nucleon electromagnetic size and for the range of the effective nucleon-nucleon interaction (2) cancel each other almost completely. The Coulomb potential was neglected since Palevsky et al.[2] have shown it to have a negligible effect over the measured region. For comparison with the WKB method, we have also evaluated the Glauber multiple-scattering series for the amplitude [Eq. (1) of Czyż and Leśniak[4]]. The two methods predict almost identical cross sections. The results, compared with experiment, are shown in Fig. 1. Agreement is quite good. A complete Glauber calculation with a more refined nuclear model has been done previously by Wilkin and Bassel[6] with much the same results. The fits in Figs. 1 and 2 are as good as those obtained by the empirical analysis of Ref. 2, which used a Wood-Saxon shape fitted to the electron elastic-scattering data, and did an exact solution of the Schrödinger equation searching on the magnitude of the real and imaginary parts of the optical potential. Since the conclusions we can draw are similar to those of Ref. 2, we merely note that there is no obvious disagreement between the electron and proton elastic scattering, and that the real part of $A$ fills up the diffraction minimum and has little effect anywhere else.

The inelastic-scattering amplitude was computed by both methods (WKB and Glauber), including the variation of $A$ with $t$. The inelastic form factors used were those obtained from the Gillet vectors for the $2^+$ and $3^-$ states of